

h. In contrast, unpalladized nanoscale ZVI (~50 g/L) resulted in <25% dechlorination over the same time period. Biphenyl was detected in both cases, suggesting complete dechlorination is possible using unmodified nanoscale ZVI. Because Aroclors are mixtures of PCB congeners, little can be determined from these experiments about the reactivity trends of individual positional isomers or between different PCB homologue groups. Because dioxinlike toxicity has been reported in coplanar PCB congeners containing both para and at least two meta substitutions (33'44', 344'5, 33'44'5, and 33'44'55') (29, 30), it is important to predict if a buildup of more-toxic coplanar congeners would result from the iron-mediated reduction of PCBs under ambient conditions.

In this study, the PCB dechlorination rate and product distributions afforded by unmodified nanoscale ZVI were measured in water/cosolvent batch reactors. No sediment or soil was used in these studies to minimize confounding factors such as PCB losses due to sorption or background contamination. The research objectives were (i) to conclusively demonstrate that nanoscale ZVI, without the addition of a noble metal such as Ni, Pt, or Pd, can dechlorinate a range of PCB congeners at ambient conditions, and (ii) to determine the relative reactivity of positional isomers within a homologue group and provide insight into structure-activity relationships that may exist. Six strategically chosen PCB congeners were used. Tetrachlorobiphenyl congener 22'45' (BZ 49) has proven resistant to microbial dechlorination in the Hudson River (3). Its more toxic coplanar isomer 33'44' (BZ 77) is present in Aroclor mixtures at concentrations 10–100 times greater than other toxic coplanar congeners (30, 31). Dechlorination of 22'35' (BZ 44) by microscale ZVI and microscale Pd/Fe⁰ at ambient temperatures has been studied (20) and provides a basis for comparing PCB reactivity in this study. Anaerobic microbial PCB dechlorination has been shown to result in a buildup of ortho-substituted dichlorobiphenyl congeners such as 22' (BZ 4) (32, 5). Comparing the reactivity of ortho-substituted noncoplanar isomers with the nonortho-substituted coplanar isomers will yield additional information about their relative reactivity. The reactivity of congener 234-trichlorobiphenyl (BZ 21), containing one ortho, meta, and para chlorine was compared with the reactivity of the di- and tetrachlorobiphenyls. Finally, the feasibility of different schemes employing nanoscale zerovalent iron for remediating PCB-contaminated sediments is discussed.

Materials and Methods

Chemicals. All PCB congeners studied (22', 34', 234, 22'35', 22'45', and 33'44'), their dechlorination byproducts, and the internal standard (22'33') were 97+% pure and obtained from Ultra Scientific (N. Kingstown, RI). Standard solutions in hexane were used for gas chromatograph (GC) calibration and neat congeners were used in batch experiments without further purification. The microscale ZVI materials tested were Fisher Scientific electrolytic powder (<100 mesh) and Peerless iron filings (8–50 mesh). Hydrochloric acid (37.6%), acetone (99.5+%), and methanol (histological grade) were used to pretreat the Peerless iron filings obtained from Fisher. Some filings were palladized using Pd(II)(CH₃CO₂)₂ (47.5 wt % Pd, Acros). Nanoscale ZVI particles were synthesized from FeSO₄·7H₂O (99.4%, Fisher) and NaBH₄ (98+%, Acros). Methanol (histological grade), sodium azide (99%), and 1,1,1,3,3,3-hexamethyldisilazane (HMDS) (98%) to silanize the serum bottles were obtained from Acros. Hexane (99.9+%), methanol (pesticide grade), and anhydrous Na₂SO₄ (10–60 mesh) used to extract PCBs from the reactors for analysis were obtained from Fisher. The Na₂SO₄ was oven-dried at 106 °C for a minimum of 4 h prior to use.

Microscale Iron Preparation. Fisher electrolytic iron was used as received. Peerless iron was treated with separate

washes of 0.37 M hydrochloric acid, acetone, and histological grade methanol using 1 mL liquid for every 2 g ZVI and dried in a 106-°C oven for 2 h under nitrogen gas. Palladized ZVI (0.05 wt %) was prepared from acid-treated Peerless iron. A 0.5 mM solution of Pd(II)C₄H₆O₄ was prepared in 1 L of histological grade MeOH. Treated Peerless iron filings (~100 g) were added and the mixture was stirred in a closed flask for 6 h on an orbital shaker at 90 rpm. The liquid was decanted and the palladized Peerless Fe(0) was oven-dried at 106 °C for 3 h under nitrogen. It is assumed that all the palladium was coated on the iron to give 0.05% Pd by weight.

Nanoscale ZVI preparation. Nanoscale ZVI was synthesized using a slightly modified method as previously described (21, 26). The primary differences between this method and previous methods are that synthesis was performed in a hood rather than in an N₂ atmosphere (except for drying), a fivefold lower FeSO₄ concentration was used (0.07 M instead of 0.36 M), a NaBH₄ solution was used instead of adding solid NaBH₄, and the particles were centrifuged and over-dried in N₂ rather than filtered from solution and vacuum-dried. The synthesis is briefly described here. Complete synthesis details are provided in the Supporting Information. Into 1 L of a 30% (volume) MeOH/deionized water solution was dissolved 20 g of FeSO₄·7H₂O. While stirring, 10 mL of 5 N NaOH aqueous solution was added dropwise to the dissolved iron solution, yielding a pH of 6.1. Next, 50 mL of a 2.1 M NaBH₄ aqueous solution was added at a rate ~0.5 mL/sec. This is approximately 2.9 times the stoichiometric amount of NaBH₄ required to reduce all the dissolved Fe²⁺ in solution to zerovalent iron. A fine black precipitate formed instantly upon addition of NaBH₄ and remained in solution throughout the process. The mixture was stirred for 20 min before being centrifuged in plastic centrifuge tubes for 5 min at 3500 rpm to separate the solids. The supernatant was discarded and the remaining solids were rinsed with MeOH twice to remove any excess salt. The nanoscale ZVI particles were then dried in a 106-°C oven for 4 h under nitrogen gas. Once dry, the particles remained in the oven for a minimum of 8 h to cool and allow oxygen to slowly bleed into the oven. This passivated the iron surface slightly and prevented the highly reactive iron particles from spontaneously igniting. The dried particles were finely ground and stored in sealed serum bottles until use. A second batch of iron was synthesized similarly, but dried in a glovebox containing 99.5% N₂/0.5% O₂ rather than pure N₂.

Nanoscale Iron Characterization. Particle size and electron diffraction patterns for the nanoscale iron were collected using a Philips EM420 transmission electron microscope (TEM) at 120 kV. The morphology of the nanoscale ZVI particles was determined using the JEM-ARM 1000 Atomic Resolution Microscope (JEOL, Ltd.) at the National Center for Electron Microscopy at Lawrence Berkeley National Laboratory. The ARM was operated at 800 kV, which allowed magnification levels of up to 1 000 000 ×. ZVI samples were dispersed (sonicated) in acetone, then dripped onto a 300-mesh Cu TEM grid with Formvar substrate or lacey carbon. The N₂-BET surface area of the nanoscale ZVI was measured using a NOVA 2200 BET-surface area analyzer (Quantachrome, Boynton Beach, FL). A five-point BET isotherm was used to determine the total available surface area of the iron. The elemental composition of nanoscale ZVI was determined by Inductively Coupled Plasma-Atomic Emission Spectrometry (ICP-AES) according to EPA Method 6010B.

Sacrificial Batch Experiments. PCB spike solutions were prepared by dissolving a known mass of neat PCB congener in acetone or methanol. The concentration of the parent compound and any unwanted PCB congeners present (i.e., impurities) in each spike solution were determined using a Hewlett-Packard 6890 gas chromatograph with an electron

TABLE 1. GC Operating Parameters

parameter	GC/ μ ECD	GC/FID	GC/MSD
column	60 m HP-5 d = 250 μ m, film = 0.25 μ m	30 m HP-5MS d = 250 μ m, film = 0.25 μ m	30 m PTE-5 d = 250 μ m, film = 0.25 μ m
carrier gas (pressure/rate)	He (20 psi)	He (2.1 mL/min)	He (1 psi)
detector gases (rate)	Ar/(5%) CH ₄ (60 mL/min)	H ₂ (45.0 mL/min) air (320.0 mL/min) He (10.0 mL/min)	N/A
detector temp	325 °C	300 °C	280 °C
inlet mode (temp/press)	splitless (250 °C/20 psi)	splitless (250 °C/21 psi)	splitless (250 °C/1 psi)
oven temperature	115 °C for 3 min, 5 °C/min	60 °C for 1 min, 20 °C/min	105 °C for 3 min, 5 °C/min
program (run time)	to 230 °C, 15 °C/min to 290 °C, 30 °C/min to 300 °C, hold 300 °C for 10 min (40 min)	to 220 °C, 30 °C/min to 280 °C, hold 280 °C for 4 min (15 min)	to 230 °C, 15 °C/min to 290 °C, 30 °C/min to 300 °C, hold 300 °C for 5 min (38 min)

capture detector (GC/ECD). An aliquot of the spike solution (~0.1 to 1 mL) was added to 500 mL of a 30 vol % methanol/water mixture to provide the desired initial PCB concentration for each experiment without exceeding the solubility limit in the water/cosolvent mixture (33). Sodium azide (~1 mM) was added to inhibit microbial activity and the solution was stirred on an orbital shaker for a minimum of 1 h prior to spiking the reactors. For each PCB congener tested, 8 reactors (12-mL amber serum bottles) were prepared by placing 2 g of iron into each bottle, adding 10 mL of solution containing the desired PCB congener, and capping with Teflon-coated rubber septa and aluminum seals. Control experiments were run identically but without addition of iron. The reactors were placed on an orbital shaker (90 rpm) or an end-over-end rotator at 20 rpm and kept at laboratory temperature (22 \pm 3 °C) until sacrificed for analysis. To minimize PCB adsorption to glass, the serum bottles were silanized in a hexane solution with 5% HMDS by volume for 1 h, rinsed with DI water, and air-dried prior to use. Approximately 2 mL of headspace remained in each bottle.

Reactors were sacrificed at predetermined times for analysis. PCB sorption to iron was significant, so both the aqueous and solid phases in each reactor were extracted to effectively search for dechlorination byproducts. Extractions were conducted in the reactor bottles without removing the septa. Experiments using microscale ZVI or Pd/Fe⁰ were extracted using the following procedure. The serum bottle was centrifuged for 5 min at 3500 rpm to separate the solid iron from the water/suspended iron. A 7-mL aliquot of the aqueous phase was withdrawn from the reactor and extracted with 0.5 mL of hexane containing 1 mg/L of the internal standard 22'33' (extraction solution) by mixing on a vortex orbital mixer. Approximately 100 μ L of the hexane extract was drawn off and added to an autosampler vial containing a 100- μ L glass insert and ~6 mg of oven-dried anhydrous sodium sulfate, and analyzed for PCBs using GC/ μ ECD. To the wet iron remaining in the bottle, approximately 1 mL of pesticide-grade MeOH was added and shaken on the vortex mixer. Next, 0.5 mL of the extraction solution (hexane/internal standard) was added and the bottle, vortexed, and analyzed for PCBs as above. Reactors containing nanoscale iron were analyzed in a similar fashion but the iron particles were not separated from the aqueous phase. Instead, 1 mL of pesticide grade methanol was added to the reactor, mixed on the vortex mixer, followed by addition of 0.5 mL of the extraction solution, shaking, and transfer to a GC vial for analysis. Experiments using microscale ZVI were conducted once. Experiments using nanoscale ZVI were repeated to verify results and assess the relative reactivity of different batches of nanoscale ZVI. Control reactors (without iron) were extracted using 0.5 mL of hexane only (no methanol).

PCB Analysis and Calibration. Analysis was by GC/ μ ECD (for PCBs), GC/FID (for biphenyl), and GC/MSD (Model

5972). The GC operating parameters for each are provided (Table 1). In all analyses, a 1- μ L aliquot of sample was injected using a Hewlett-Packard liquid autosampler (Model 18593B). These operating parameters provided excellent separation of the PCB congeners used as well as of the dechlorination byproducts, except where noted. When necessary, the identities of PCB dechlorination byproducts were verified with GC/MSD. The detector was tuned using the standard spectra autotune to compare the mass spectra with the NIST/EPA/NIH Chemical Structures Database (library NBS75K.L) with >90% quality.

The GC/ μ ECD was calibrated for all PCB congeners tested and all potential dechlorination products using 22'33' as an internal standard (IS). Response factors were determined for each congener and the internal standard. Regressions ($R^2 > 0.99$) were determined from a three-point calibration of biphenyl, a three-point calibration of monochlorobiphenyls, a four-point calibration of dichlorobiphenyls, and either a four or five-point calibration for tri- and tetrachlorobiphenyls. The approximate detection limits were 1 nmol for biphenyl and 3-chlorobiphenyl, 0.1 nmol for 2, 4, 22', 33', and 34', and 0.01 nmol for all other congeners.

In experiments using 22'45', the potential byproducts 22'5 and 34' (resulting from loss of the ortho chlorines) coelute. It was assumed that no 34' was formed due to loss of the ortho chlorines and only 22'5 constituted the peak at 27.9 min. In experiments with Pd/Peerless Fe⁰, it was assumed congeners 24 and 25 coeluted and had the same response (i.e., each congener made up half of the peak area).

System Mass Balance. The mass balance at each sampling event was calculated as the ratio of the total PCB congeners measured to the initial PCB mass measured in the system

$$MB (\%) = \frac{\left(\sum M_i \right)}{M_{o, t=0}} \times 100 \quad (1)$$

where M_i is the mass of all PCBs in solution at time t including all dechlorination byproducts and the parent compound, and $M_{o, t=0}$ is the mass of the parent congener at the initial sampling event in μ mol. In experiments where aqueous and iron phases could be separated, PCB masses in the aqueous and iron extracts were summed to calculate the total mass in the reactor.

PCB Dechlorination Rate Constants. The pseudo-first-order PCB dechlorination rate constants were determined from the rate of product formation rather than loss of the parent congener. This is primarily because (i) conversion of the parent PCB congener over the 1.5-to-6-month reaction time was low (40% or less), (ii) nondestructive loss of mass of the parent PCB compound due to irreversible sorption is likely, and (iii) no products were observed in control reactors without iron. The observed pseudo-first-order rate constants

TABLE 2. Iron Physical and Chemical Properties

	particle size (nm)	N ₂ BET—surface area (m ² /g)	elemental composition (wt %)
nanoscale ZVI	30–50 (~1 μm aggregates)	36.5	Fe 60 B 4 O 36 ^a
fisher electrolytic iron	< 150 000 (< 100 mesh)	0.18 ^b	Fe > 99
peerless iron	2 300 000 < d _p < 300 000 (8 to 50 mesh)	1.23 ^b	Fe 98 C ~2 ^c

^a Only Fe and B were measured. The balance of the composition is assumed to be O in the Fe–oxide shell. The presence of O has been qualitatively determined using EDX and no other elements were detected in the particles. ^b Alowitz and Scherer (44). ^c From Peerless product information sheet.

were calculated from fits of the products formed in each reactor using eq 2

$$-\frac{dM_i}{dt} = \frac{d \sum \text{Products}}{dt} = k_{\text{obs}} M_i \quad (2)$$

where M_i is the mass of the parent PCB congener, $\sum \text{products}$ is the sum of all observed products, and k_{obs} is the observed pseudo-first-order rate constant. Fits were performed using a kinetic modeling software package, Scientist, v. 2.01 (Micromath, St. Louis, MO). Reported errors are 95% confidence intervals for these fits. All product data was used for the nanoiron experiments. Products data collected prior to deactivation ($t < 3$ days) was used to calculate PCB dechlorination rates using Pd/Fe.

Results

Iron Characterization. TEM images of the N₂-dried nanoscale ZVI particles (before reaction) are shown in Figure 1a and 1b. The N₂-BET surface area and elemental composition of all particles used in this study are provided in Table 2. The nanoscale ZVI exists as aggregates of spherical particles averaging 30–50 nm in diameter. The specific surface area of nanoscale ZVI particles is ~2 orders of magnitude greater than for the microscale iron particles. Assuming spherical particles and identical densities for each type of iron, the 40-nm-diameter nanoscale ZVI particles should have approximately a 4 order of magnitude larger surface area-to-volume ratio ($3/R$) than the other particle types, so the measured surface area of 36.5 m²/g is not unreasonable. It is also consistent with previously reported measurements (21, 26, 27). The nanoscale ZVI particles appear to have a core–shell morphology (Figure 1b). The particles contain ~60 wt % iron and ~4 wt % boron, also consistent with other reported studies (26). The remaining 36 wt % of the particle mass is presumed to be atomic oxygen in Fe–oxides. The d spacings for electron diffraction patterns [0.201 nm (110), 0.119 nm (211), and 0.145 nm (200)] are consistent with d spacings for the three strongest reflections of bcc Fe⁰ [0.203 nm (110), 0.117 nm (211), and 0.143 nm (200)] indicating that α-Fe(0) is present in the particles. The presence of oxygen atoms was verified qualitatively using EDX and no other elements were present in substantial quantities. It is therefore likely that the core of these particles is α-Fe(0) while the shell consists mostly of Fe–oxide. Nanoscale ZVI synthesized in a similar fashion had an enrichment of boron (oxidized) in the surface layers (~11%) (26). It is assumed that the boron distribution and speciation in these particles is similar. The nature and extent that boron influences particle reactivity is unclear and is under investigation.

PCB Dechlorination Rates Using Different forms of ZVI.

No products formed in control reactors without iron. No PCB dechlorination products were observed in batch reactors with microscale Fisher electrolytic iron powder or Peerless Fe⁰ filings after 180 days, suggesting that these forms of iron are not reactive. Quantifiable PCB dechlorination products

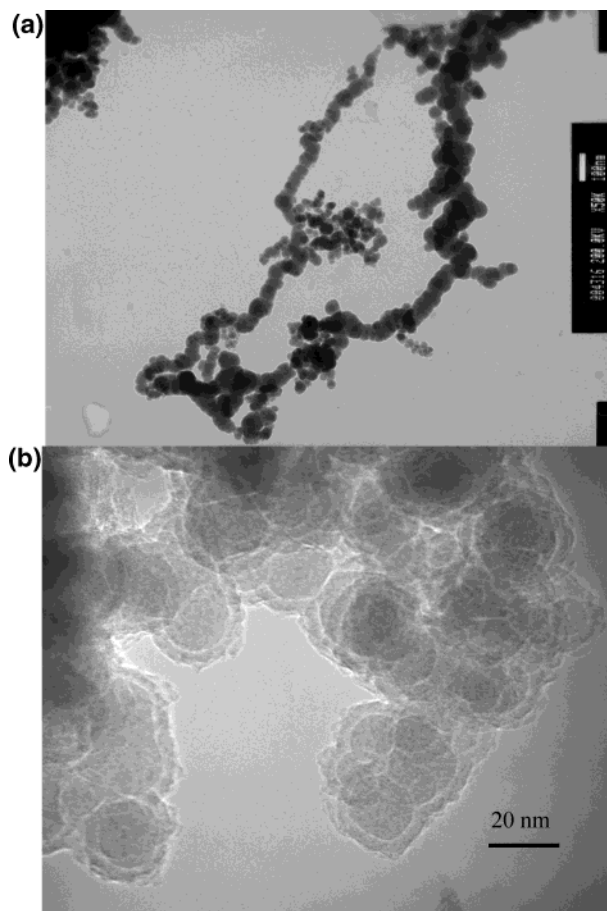


FIGURE 1. (a) Aggregate spherical particles of nanoscale ZVI (50 000×). (b) Core–shell morphology of nanoscale ZVI particles (250 000×).

were formed in reactors containing Pd/Peerless Fe⁰ and nanoscale ZVI. Figure 2 shows the byproduct distributions from dechlorination of 22'35' with Pd/Peerless Fe⁰. Figure 3 shows the total mass of the products formed during dechlorination of each of the congeners evaluated by unmodified nanoscale ZVI, and the corresponding data fits using eq 2. Figure 4 shows the loss of 33'44' and byproducts formed during dechlorination using unmodified nanoscale ZVI, along with the corresponding data fits using eq 2. The surface-area-normalized PCB dechlorination rate constants and corresponding reactor-specific half-lives for all PCB congeners tested are provided in Table 3. The dechlorination rate constants in Table 3 were all determined using the same ZVI (glovebox-dried) so the reactivity of different congeners is directly comparable.

System Mass Balance. Mass balances for PCBs were calculated for all experiments. It is assumed that the extraction efficiencies were the same for all PCB congeners. PCB mass

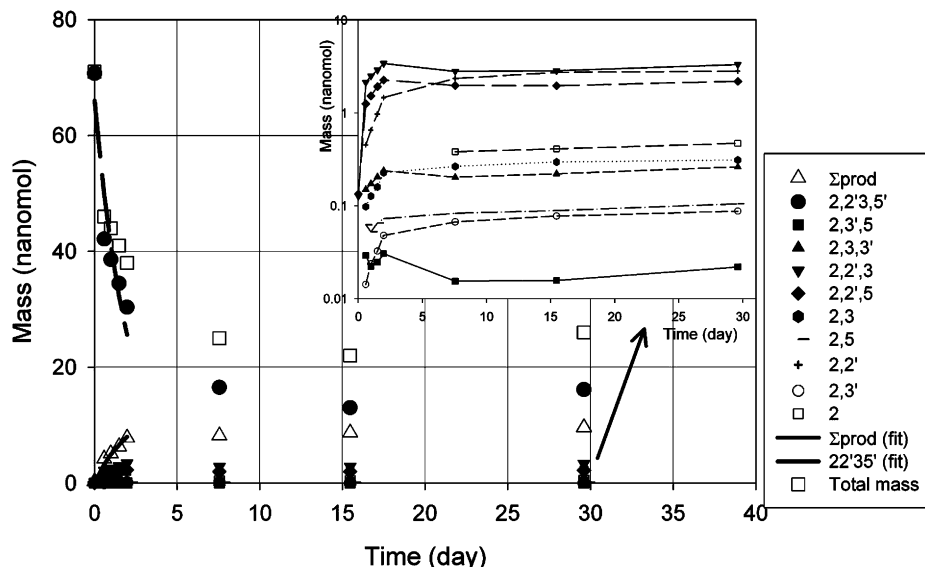


FIGURE 2. Byproduct distribution during dechlorination of PCB congener 22'35' using Pd/Peerless Fe⁰ (0.05 wt % Pd). Lines on larger plot are data fits using eq 2. Lines on inset are interpolated (not data fits) and only meant to guide the eye.

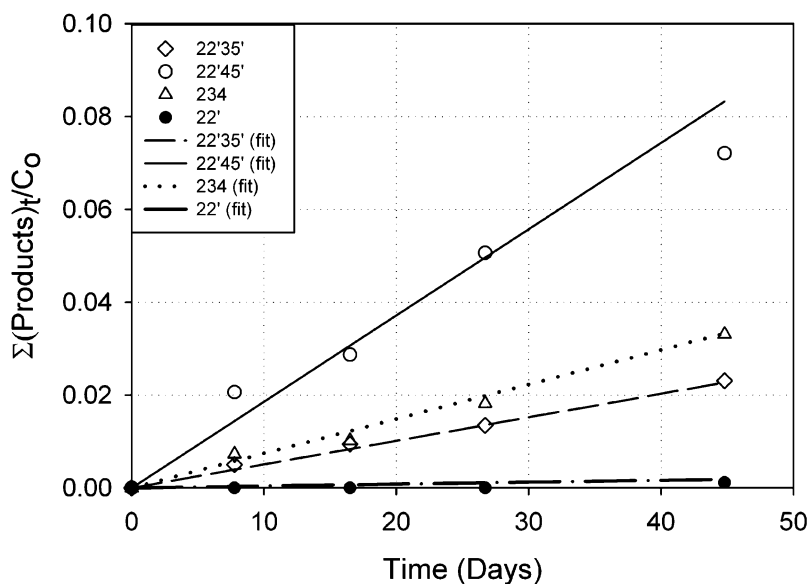


FIGURE 3. Byproduct distribution during dechlorination of PCB congeners 22'35', 22'45', 234, and 2,2' using glovebox-dried (99.5% N₂/0.5% O₂) nanoscale ZVI. Lines represent data fits using eq 2.

balances in experiments with Pd/Peerless Fe⁰ ranged from 36 to 70%. PCB mass balances with Fisher electrolytic iron, which lacks carbon inclusions, were higher at 50–90%. PCB mass balances of 56–104% were obtained in nanoscale ZVI experiments. With Peerless Fe⁰ that is 2% carbon, PCBs may not have been efficiently extracted from these carbon inclusions, resulting in poor mass balances after 4 days. Because PCBs are likely to undergo stepwise reductive dechlorination with ZVI (23, 24), the formation of soluble reaction products that would not be measured with GC/ μ ECD is doubtful. During the experiment, a small fraction of PCBs would have volatilized into the headspace. Using estimates of Henry's constant (34), this fraction is \ll 1% and does not account for the total mass deficit. Microbial degradation is doubtful owing to the presence of NaN₃. By using amber glass, the likelihood of PCB photodegradation is small. Preliminary studies showed less PCB sorption to glass reactors that were silanized, but sorption was not eliminated as has been documented in other studies (35). Control reactors that lacked iron also showed some loss of the spiked PCB congener (up to 50%), but no products were

formed. The less than 100% mass balance observed in these experiments is therefore likely due to irreversible sorption of the parent congener to glassware and the Teflon-lined septa. It should be noted that nondestructive loss of the dechlorination products would bias the observed dechlorination rate constants reported here toward underestimating the actual PCB dechlorination rate constants, however, the order of magnitude differences in the observed rates (e.g., 22' vs 34' and 22'35'/2,2'4,5' and 33'44') exceed the potential error due to nondestructive mass loss of PCB dechlorination products.

Discussion

Microscale ZVI. The lack of reactivity of microscale ZVI (Fisher and Peerless) after 180 days is reasonable considering that its surface area is \sim 2 orders of magnitude lower than that of nanoscale ZVI. It has been demonstrated that the ZVI-promoted reaction rate is first order with respect to the iron surface area (36). The surface-area-normalized PCB dechlorination rate constant for 33'44' using nanoscale ZVI is $5.5 \pm 1.4 \times 10^{-4} \text{ yr}^{-1} \text{ m}^{-2} \text{ L}$. Based on this rate constant, the

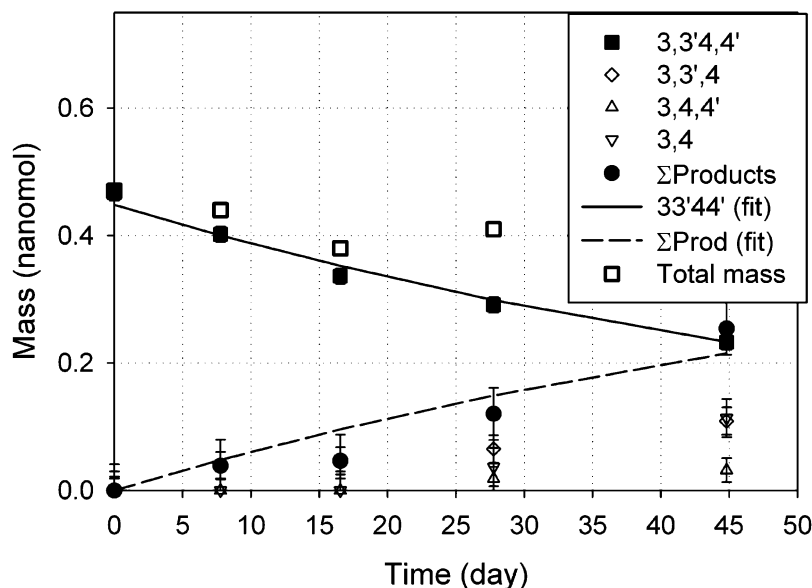


FIGURE 4. Loss of parent compound and byproduct distribution during dechlorination of toxic, coplanar PCB congener 33'44' using glovebox-dried (99.5% N₂/0.5% O₂) nanoscale ZVI. PCB mass balance is 104%. Lines represent data fits using eq 2.

TABLE 3. Measured Surface Area normalized PCB Dechlorination Rate Constants and Reactor-Specific Half-Life Times

congener	0.05 wt % Pd/Fe ⁰		nanoscale ZVI ^a	
	$k_{\text{obs}} 10^2$ (L yr ⁻¹ m ⁻²)	$t_{1/2}$ (yr)	$k_{\text{obs}} 10^5$ (L yr ⁻¹ m ⁻²)	$t_{1/2}$ (yr)
22'	3.8 ± 1.4	0.07	0.1 (est.) ^c	77
34'	17 ± 10	0.02	1.8 ± 1.8	5.3
234	5 ± 2	0.06	3.7 ± 0.4	2.6
22'35'	14 ± 5	0.02	2.6 ± 0.1	3.6
22'45'	12.6 ± 6	0.02	9.3 ± 0.1	1.0
33'44'	ND ^b	ND	55 ± 14	0.2

^a Glovebox-dried Nanoscale ZVI. ^b Not determined. ^c Estimated from trace of 2-CBP observed. Reported errors are 95% confidence intervals for pseudo-first-order fit of product data (eq 2).

expected pseudo-first-order rate constant for 33'44' in a reactor containing 200 g L⁻¹ of Peerless Fe⁰ (N₂-BET surface area = 1.23 m²/g) is 0.14 ± 0.03 yr⁻¹. Given this rate constant, some PCB dechlorination products (~10% of the initial PCB mass) should have been measurable after 180 days had Peerless Fe⁰ been capable of dechlorinating PCBs. No byproducts were observed in reactors containing 33'44' and unmodified Peerless Fe⁰, suggesting that factors other than iron surface area prevented PCB dechlorination from occurring. The fastest observed PCB dechlorination rates were achieved using Pd/Peerless Fe⁰. These rates are similar to previously reported rates by palladized iron (20). Palladium likely serves as a catalyst, lowering the activation energy of the reaction (25). The rapid dechlorination rate, however, is only sustained for 2 days (Figure 2). After this initial period, the reactivity appears to cease in all experiments and product levels remain unchanged for a month. This trend was observed for all experiments using Pd/Peerless Fe⁰. A similar trend was noted in a previous study using 0.25 wt % Pd/Fisher electrolytic (<40 mesh) iron but was not discussed (20). Loss of reactivity could result from passivation of the palladium surface or poisoning (37). Assuming a historical bulk iron cost of \$350/ton and a bulk Pd market price of \$14.75/gram, the additional materials cost of palladized ZVI filings (at 0.05 wt %) to unpalladized ZVI is approximately 20:1. The use of palladized iron for PCB remediation is not

likely to be economical given the cost and the current inability to provide long-term dechlorination rate enhancement.

Nanoscale ZVI. Nanoscale ZVI had a greater specific surface area than microscale iron and was more reactive. Additionally, gas bubbles (likely H₂) were observed in these reactors but not with the microscale iron. The high surface-to-volume ratio and the rapid formation of hydrogen gas may have enabled nanoscale ZVI to dechlorinate PCBs during the 45-day experiment. The presence of B (4 wt %, ~18 at. %) may also play a role if an Fe-B alloy or Fe-B-oxide is formed that significantly alters the electronic properties of the oxide shell. It is also possible that the nanoiron reactivity (compared to microscale iron) is due to the small particle size. The observed primary particle size (~50 nm) of Fe/B is probably not small enough to increase the Fermi potential and lower the potential of the Fe²⁺/Fe⁰ redox couple, as has been reported for silver nanoparticles with low aggregation numbers (ca. < Ag₁₀₀) (38), but size effects may be possible if the 50-nm particles are in fact aggregates of very fine clusters of Fe⁰ atoms with similarly low aggregation numbers.

While the data set collected here is not extensive enough to support strong conclusions regarding structure-activity relationships, some general trends are apparent. Considering PCB congeners containing two ortho chlorines (22', 22'35', and 22'45'), the dechlorination rate increased with increasing chlorine substitution. Much less variability in the PCB dechlorination rate was observed with the Pd/Peerless Fe⁰. Furthermore, nonortho-substituted congeners are significantly more reactive than their ortho-substituted isomers (34' vs 22' and 33'44' vs 22'35'/22'45'). The highest chlorinated, nonortho-substituted congener (33'44') was dechlorinated faster and to a greater extent than any other congener studied. The reactivity of the trichloro-PCB congener (234) was similar to a dichloro nonortho-substituted congener (34') and a tetrachloro diortho-substituted congener (22'35'). This congener contains one ortho chlorine rather than two, so its relative reactivity may be affected by both the number of chlorine substitutions and the number of ortho chlorines. The number of orthochlorines present on congeners may affect reactivity because the torsion angles between the biphenyl ring increases with increasing ortho substitution, 38° (nonortho), 58° (mono-ortho), and 73° (di-ortho) when they are sorbed (39). Nonortho-substituted congeners may be able to adsorb in a closer planar position with iron, which

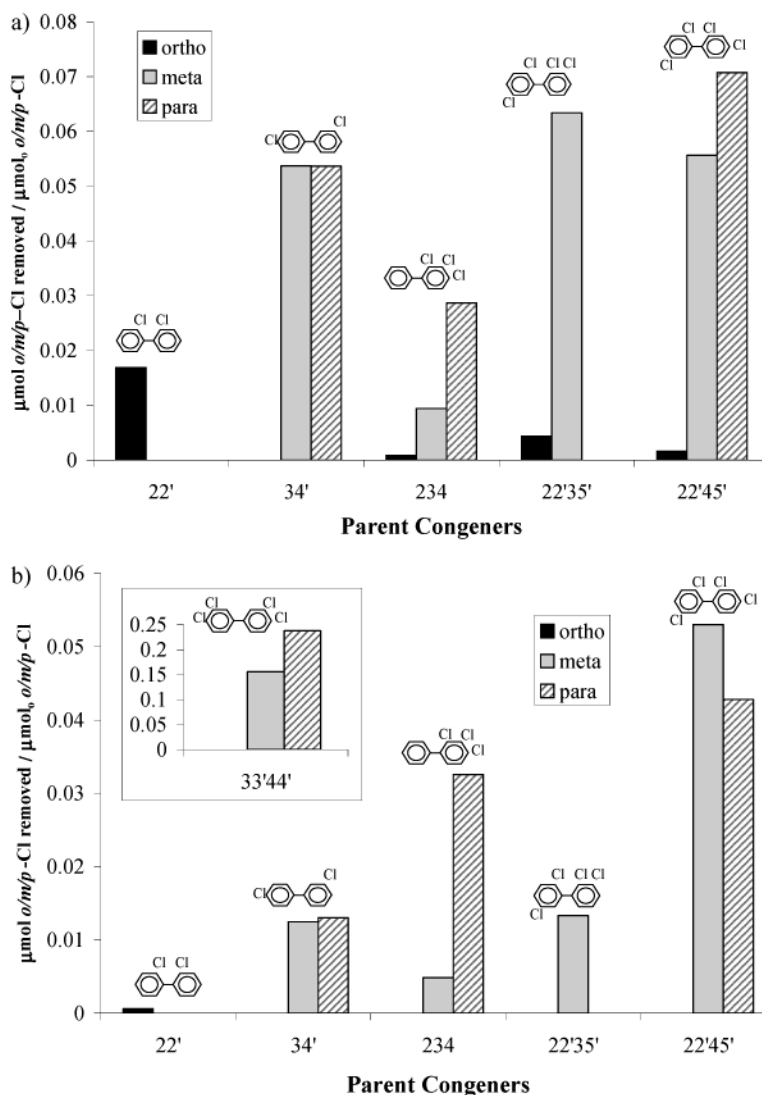


FIGURE 5. (a) Chlorine removal patterns after 2 days with 0.05% Pd/Peerless Fe(0). (b) Chlorine removal patterns after 45 days with glovebox-dried nanoscale ZVI.

may be more favorable for reductive dechlorination. The increased reactivity of higher-chlorinated PCB congeners and nonortho-substituted congeners correlates with the more positive reduction potentials measured in previous studies for such congeners (40–43). These observations suggest that (1) the measured reduction potentials may be useful in predicting trends in the dechlorination rate constants of PCBs using nanoscale ZVI, (2) higher-chlorinated congeners should dechlorinate faster than lower-chlorinated congeners, and (3) nonortho-substituted congeners should dechlorinate faster than their ortho-substituted isomers.

Effect of Iron Drying Atmosphere. The dechlorination rate constant for 22'35' using N₂-dried nanoscale ZVI was 2.3 yr⁻¹ with a half-life of 0.3 years (data not shown). For glovebox-dried nanoscale ZVI, the dechlorination rate constant for 22'35' was only 0.19 yr⁻¹ with a half-life of 3.6 years (Table 2). The decrease in reactivity of glovebox-dried nanoscale ZVI is likely due to the formation of a less-active or thicker oxide layer during drying (Figure 1b). Thus, the synthesis method of the nanoscale ZVI particles, and exposure to oxygen, can affect the particle reactivity. The dechlorination product distribution, however, was the same regardless of the iron synthesis/drying technique so conclusions regarding potential dechlorination products are unaffected.

Positional Isomer Reactivity. The relative masses of ortho, meta, and para chlorines that were removed after 2 days for

each PCB congener with Pd/Peerless Fe⁰ are given in Figure 5a. Based on byproduct formation from dechlorination of tri- and tetrachlorobiphenyls, meta and para chlorine removal was dominant but some ortho dechlorination did occur. Furthermore, para chlorines may be preferentially removed over meta chlorines for 234 and 22'45'. For the dichlorobiphenyls, some ortho dechlorination was observed with 22'. Nearly equal fractions of meta and para chlorine removal occurred with 34'. For Pd/Peerless Fe⁰, nonortho chlorines (para or meta) are preferentially removed over ortho chlorines when both are present, but ortho dechlorination is possible. No biphenyl was observed in these systems, suggesting that complete dechlorination is not likely at the low Pd loading used (0.05 wt % Pd). This is consistent with previous observations (20).

Similar data for PCB dechlorination after 45 days using glovebox-dried nanoscale ZVI are shown in Figure 5b. In the ortho-substituted tri- and tetrachlorobiphenyls, meta and para chlorine removal was dominant as no ortho dechlorination occurred after 45 days. Para chlorines may be preferentially removed over meta chlorines. Ortho chlorines were removed from 22', but only trace amounts of products were identified.

These results suggest that Pd/Peerless Fe⁰ and nanoscale ZVI tend to dechlorinate PCBs in a predictable manner with chlorine removal from each position following the general

trend para \geq meta \gg ortho chlorines. This is consistent with results from previous studies. The dechlorination products measured by West et al. (20) using 22'35' and 0.25%-Pd 40-mesh iron also suggest that ortho chlorines are more resistant to removal than meta chlorines. Yak et al. (24), who investigated PCB dechlorination by microscale ZVI in sub-critical water at 250 °C, found ortho-substituted congeners were less likely to undergo reductive dechlorination than meta or para-substituted congeners. Furthermore, they found meta chlorines more resistant to removal than para chlorines (24). For example, they estimated the ratio of 33'4/344' from the dechlorination of 33'44' to be 3/2. For nanoscale ZVI under ambient temperatures in this study, this ratio is 7/2. Thus abiotic, nanoscale ZVI-mediated PCB dechlorination should result in byproducts that have lower fractions of para and meta chlorines but a higher fraction of ortho chlorines. This is favorable because ortho-substituted PCB congeners are less toxic than non ortho-substituted, coplanar PCB congeners.

Engineering Implications. It is encouraging that reactivity was noted with all the congeners studied and does offer some promise that nanoscale ZVI could dechlorinate all 209 congeners. Coating microscale iron with palladium makes microscale iron reactive, but the rate enhancement is short-lived and does not justify using the expensive catalyst unless the catalytic activity can be sustained or if the Pd/Fe⁰ media can be regenerated in situ. This will be difficult and cost prohibitive in large-scale field applications. The slow rates of dechlorination with nanoscale ZVI require it to be in prolonged contact with the PCBs. Thus, ex situ treatment reactors for PCB-contaminated waste streams (e.g., effluent from soil/sediment washing processes) requiring rapid dechlorination rates are not likely to be practical. Dechlorination of PCBs with nanoscale ZVI may, however, be possible in situ (e.g., mixing nanoscale ZVI into PCB-contaminated sediments stored in confined disposal facilities (CDF) or in diffusion-dominated systems such as a reactive barrier covering contaminated sediments left in place). PCBs in natural media are predominantly sorbed to solids rather than in solution, so the PCB dechlorination rates achievable in situ applications will ultimately be limited by the PCB desorption rate and subsequent transport to a reactive nanoiron particle. The presence of competing substrates, dissolved solids, dissolved oxygen, etc. will also affect the PCB dechlorination rate. The physical processes limiting the availability of PCBs to iron will have to be considered in any remedial design. Currently, the cost of producing nanoscale ZVI by methods described here (~ \$200–300 per kg) is too high for widespread application in sediments, but these costs are expected to decrease as the market for nanoscale ZVI increases and alternative synthesis processes become available. Methods to cost-effectively synthesize nanoscale ZVI must become available, and the long-term reactivity of nanoscale ZVI under natural reaction conditions must be assessed, before this technology becomes a viable approach for remediating PCBs in situ.

Acknowledgments

This research was supported in part by the Hazardous Substance Research Center (HSRC) South and Southwest through a research Grant to Dr. Lowry (R139634), the National Science Foundation through a Graduate Student Fellowship to K.M.J., and Alcoa, Inc. The authors also thank Dr. Christopher S. Kim and the National Center for Electron Microscopy (NCEM) for providing the ARM images and Dr. Dorothy Farrell for the TEM and electron diffraction images.

Supporting Information Available

Detailed synthesis steps for the nanoscale iron used in this study. This material is available free of charge via the Internet at <http://pubs.acs.org>.

Literature Cited

- (1) *A Risk Management Strategy for PCB—Contaminated Sediments*; National Research Council, National Academy Press: Washington DC, 2001.
- (2) *Superfund Proposed Plan: Hudson River PCBs Superfund Site*, New York; U.S. EPA Region 2; Dec 2000, p 26.
- (3) Rhee, G.-Y.; Sokol, R. C.; Bush, B.; Bethoney, C. M. *Environ. Sci. Technol.* **1993**, *27* (4), 714–719.
- (4) Wiegel, J.; Wu, Q. *FEMS Microbiol. Ecol.* **2000**, *32*, 1–15.
- (5) Zwiernik, M. J.; Quensen, J. F., III; Boyd, S. A. *Environ. Sci. Technol.* **1998**, *32* (21), 3360–3365.
- (6) Cutter, L.; Watts, J.; Sowers, K.; May, H. D. *Environ. Microbiol.* **2001**, *3* (11), 699–709.
- (7) Wu, Q.; Watts, J.; Sowers, K.; May, H. D. *Appl. Environ. Microbiol.* **2002**, *68* (2), 807–812.
- (8) Fish, K. M.; Principe, J. M. *Appl. Environ. Microbiol.* **1994**, *60* (12), 4289–4296.
- (9) Abramowicz, D. A.; Brennan, M. J.; Van Dort, H. M.; Gallagher, E. L. *Environ. Sci. Technol.* **1993**, *27* (6), 1125–1131.
- (10) Master, E. R.; Lai, V. W.; Kuipers, B.; Cullen, W. R.; Mohn, W. M. *Environ. Sci. Technol.* **2002**, *36* (1), 100–103.
- (11) Dingyi, Y.; Quensen, J. F., III; Tiedje, J. M.; Boyd, S. A. *Appl. Environ. Microbiol.* **1992**, *58* (4), 1110–1114.
- (12) Natarajan, M. R.; Nye, J.; Wu, W.-M.; Wang, H.; Jain, M. K. *Biotech. Bioeng.* **1997**, *55* (1), 182–190.
- (13) Williams, W. A.; May, R., J. *Environ. Sci. Technol.* **1997**, *31* (12), 3491–3496.
- (14) Han, S.; Eltis, L. D.; Timmis, K. N.; Muchmore, S. W.; Bolin, J. T. *Science* **1995**, *270* (5238), 976–980.
- (15) Matheson, L. J.; Tratnyek, P. G. *Environ. Sci. Technol.* **1994**, *28* (12), 2045–2053.
- (16) Vogar, J. L.; Focht, R. M.; Clark, D. K.; Graham, S. L. *J. Hazard. Mater.* **1999**, *68* (1), 97–108.
- (17) Gillham, R. W.; O'Hannesin, S. F. *Ground Water* **1994**, *32*, 958–967.
- (18) Eykholt, G.; Davenport, D. *Environ. Sci. Technol.* **1998**, *32* (10), 1482–1487.
- (19) Powell, R. M.; Powell, P. D.; Puls, R. W. *Economic Analysis of the Implementation of Permeable Reactive Barriers for Remediation of Contaminated Groundwater* EPA/600/R-02/034; Environmental Protection Agency, U.S. Office of Research and Development: Cincinnati, June 2002.
- (20) West, O. R.; Liang, L.; Holden, W. L.; Korte, N. E.; Fernando, Q.; Clausen, J. L. *Degradation of Polychlorinated Biphenyls (PCBs) Using Palladized Iron*; ORNL/TM-13217; Oak Ridge National Laboratory: Oak Ridge, TN, 1996; 37831.
- (21) Wang, C.; Zhang, W. *Environ. Sci. Technol.* **1997**, *31* (7), 2154–2156.
- (22) Chuang, F.; Larson, R. A.; Wessman, M. S. *Environ. Sci. Technol.* **1995**, *29* (9), 2460–2463.
- (23) Yak, H. K.; Wenclawiak, B. W.; Cheng, I. F.; Doyle, J. G.; Wai, C. M. *Environ. Sci. Technol.* **1999**, *33* (8), 1307–1310.
- (24) Yak, H. K.; Lang, Q.; Wai, C. M. *Environ. Sci. Technol.* **2000**, *34* (13), 2792–2798.
- (25) Grittini, C.; Malcomson, M.; Fernando, Q.; Korte, N. *Environ. Sci. Technol.* **1995**, *29* (11), 2898–2900.
- (26) Schrick, B.; Blough, J. L.; Jones, D.; Mallouk, T. E. *Chem. Mater.* **2002**, *14*, 5140–5147.
- (27) Zhang, W. X. *J. Nanopart. Res.* **2003**, *5*, 323–332.
- (28) Ponder, S. M.; Darab, J. G.; Mallouk, T. E. *Environ. Sci. Technol.* **2000**, *34* (12), 2564–2569.
- (29) Safe, S. *Crit. Rev. Toxicol.* **1990**, *21* (1), 51–88.
- (30) Safe, S. *Crit. Rev. Toxicol.* **1994**, *24* (2), 87–149.
- (31) Frame, G. M.; Cochran, J. W.; Boewadt, S. S. *J. High Resolut. Chromatogr.* **1996**, *19*, 657–668.
- (32) Alder, A. C.; Häggblom, M. M.; Oppenheimer, S. R.; Young, L. Y. *Environ. Sci. Technol.* **1993**, *27* (3), 530–538.
- (33) Morris, K. R.; Abramowitz, R.; Pinal, R.; Davis, P.; Yalkowsky, S. H. *Chemosphere* **1988**, *17* (2), 285–298.
- (34) Shiu, W. Y.; Mackay, D. J. *Phys. Chem.* **1986**, *15* (2), 911–929.
- (35) Poerschmann, J.; Górecki, T.; Kopinke, F.-D. *Environ. Sci. Technol.* **2000**, *34* (17), 3824–3830.
- (36) Johnson, T. L.; Scherer, M. M.; Tratnyek, P. G. *Environ. Sci. Technol.* **1996**, *30* (8), 2634–2640.
- (37) Lowry, G. V.; Reinhard, M. *Environ. Sci. Technol.* **2000**, *34* (15), 3217–3223.
- (38) Mostafavi, M.; Marignier, J.; Amblard, J.; Belloni, J. *Radiat. Phys. Chem.* **1989**, *34* (4), 605–617.
- (39) Jakuš, V.; Miertuš, S. *Chem. Pap.* **1990**, *44* (5), 589–601.

- (40) Huang, Q.; Rusling, J. F. *Environ. Sci. Technol.* **1995**, *29* (1), 98–103.
- (41) Farwell, S. O.; Beland, F. A.; Geer, R. D. *Electroanal. Chem. Interface Electrochem.* **1975**, *61*, 315–324.
- (42) Connors, T. F.; Rusling, J. F.; Owlia, A. *Anal. Chem.* **1985**, *57*, 170–174.
- (43) Rusling, J. F.; Miaw, C. L. *Environ. Sci. Technol.* **1989**, *23* (4), 476–479.

- (44) Alowitz, M. J.; Scherer, M. M. *Environ. Sci. Technol.* **2002**, *36* (3), 299–306.

Received for review February 1, 2004. Revised manuscript received June 18, 2004. Accepted July 7, 2004.

ES049835Q